

Contents lists available at ScienceDirect

Tetrahedron

journal homepage: www.elsevier.com/locate/tet



Cerium(IV) based oxidative free radical cyclization of active methylene compounds with some cyclic alkenes: A useful annulation method for terpene functionalization



Jan Světlík ^{a, **}, František Tureček ^b, Katarzyna Hartwich ^c, Krzysztof Kozieł ^c, Paweł Pakulski ^c, Aleksandra Pałasz ^c, Justyna Kalinowska-Tłuścik ^c, Dariusz Cież ^{c, *}

- ^a Department of Pharmaceutical Analysis and Nuclear Pharmacy, Faculty of Pharmacy, Comenius University in Bratislava, Odbojarov 10, 832 32 Bratislava, Slovakia
- ^b Department of Chemistry, Bagley Hall, Box 351700, University of Washington, Seattle, WA, 98195-1700, USA
- ^c Department of Chemistry, Jagiellonian University, Gronostajowa 2, 30-387, Kraków, Poland

ARTICLE INFO

Article history:
Received 17 January 2019
Received in revised form
21 March 2019
Accepted 22 March 2019
Available online 27 March 2019

Keywords: Cyclization Radicals CAN Terpenes Stereoselectivity Mechanism

ABSTRACT

Ceric ammonium nitrate-mediated oxidative cyclizations of CH-acids with terpenes and terpene like substrates were investigated. Dimedone, acetylacetone, and methyl nitroacetate were condensed with pinene, norbornene, nopol, camphene, and carvone and the reaction stereoselectivity was examined. Condensation with endocyclic double bonds in pinene and nopol displayed stereoselectivity, resulting in the formation of pure enantiomers. Condensation with exocyclic double bonds in camphene and carvone produced enantiomer mixtures. The mechanism of the intramolecular annulation in a nopol derivative is discussed with the help of DFT and ab initio calculations.

© 2019 Elsevier Ltd. All rights reserved.

1. Introduction

Alkene difunctionalization by oxidative free radical cyclization of CH-acids with unsaturated compounds has become a useful method for a one-pot preparation of various heterocyclic systems. Heiba, Dessau [1] and Kurz [2] have reported that various active-methylene compounds can be oxidized to reactive radicals by high-valent metal salts, including the strong one-electron oxidant diammonium cerium(IV) nitrate (ceric ammonium nitrate, CAN). Baciocchi and coworkers have used this reactant for the generation of free radicals from carbonyl compounds and investigated their oxidative additions to 1,3-butadiene [3], as well as vinyl [4] and isoprenyl acetates [5]. Oxidative couplings of β -dicarbonyl CH-acids via radical intermediates with alkenes [6], chalcones [7] and other

E-mail addresses: svetlik@fpharm.uniba.sk (J. Světlík), ciez@chemia.uj.edu.pl (D. Cież).

enones [8], methacrylates, and analogous α , β -unsaturated esters [9] have provided a convenient route to substituted dihydrofurans. The further development of this procedure gave an easy access to β -lactams [10], highly substituted pyrroles [11] and isoxazoline Noxides [12].

Oxidative free radical additions of β -dicarbonyl CH-acids to double C=C bonds usually result in mixtures of stereoisomers. However, stereoselective reactions have been reported in some instances, for example, the formation of *exo* and *endo* adducts from intramolecular cyclization of nitroalkenes [13], *gluco* and *manno* diastereomers by addition of nitroacetates to unsaturated carbohydrates [12], stereoselective synthesis of spiro products [8], and *cis-trans* isomers prepared by reactions of CH-acids with chalcones [7]. In contrast, our survey of the literature has revealed only one article describing diastereoselective addition of CH-acids to chiral dienes [14].

Stereochemical control of chemical reactions often relies on preexisting stereogenic centers that determine the preferential formation of new stereogenic centers. Cyclic molecules, in particular, can offer limited conformational freedom or fixed conformations

^{*} Corresponding author.

^{**} Corresponding author.

that enhance stereoselectivity. To also control absolute configuration of the new chiral centers, unsaturated terpenes and terpenelike molecules appear to be the substrates of choice. They represent a ubiquitous class of naturally occurring compounds found in the plant kingdom and serve as a pivotal starting material for the production of medicines, flavors and fragrances [15]. In addition, carbocyclic terpenes and their derivatives have been utilized as valuable sources of chiral building blocks [16]. Because of their amazing diversity, monoterpenes furnish several types of acyclic, monocyclic, bridged bicyclic and tricyclic compounds, many of which are commercially available, cheap and often delivered in enantiomerically pure form. Furthermore, it has been demonstrated that some of those natural products possess anticarcinogenic properties, acting at different cellular and molecular levels and are currently under evaluation in clinical trials [17]. Therefore these substances might become a promising agent in the chemoprevention and chemotherapy of cancer [18]. These characteristics motivated the present study that is focused on the functionalization of selected monoterpenes and related cyclic compounds. Here, we report on the CAN induced [3 + 2] annulative process between compounds possessing active methylene moiety and selected terpene-type molecules, with particular emphasis on the aspects of stereoselectivity. We also explore an intramolecular version of the cyclization reaction that we utilize for the elucidation of the reaction mechanism and radical intermediates using electronic structure theory calculations.

2. Results and discussion

2.1. Cyclizations with (1S)-(-)- α -pinene

We began our investigations with (1S)-(-)- α -pinene **1** as a chiral, sterically hindered alkene. It may be supposed that the oxidative radical cyclizations of CH-acids with this natural terpene bearing an endocyclic double bond should, in principle, proceed highly stereoselectively. Two readily available CH-acids - dimedone 2a and ethyl nitroacetate **2b** were chosen for the planned purposes. CANmediated reactions were performed in methanol where the reagent is well soluble. In contrast, attempts at reacting CAN in acetonitrile were unsuccessful and yielded complex mixtures of unidentified products. Oxidative annulation of dimedone **2a** with (1S)-(-)- α pinene 1 in methanol gave an oily, yellowish product 3a in good yield. HPLC chromatogram showed that the compound 3a was formed as a pure diastereomer. The IR spectrum displayed two absorption bands at 1726 and 1617 cm⁻¹ belonging to the stretching vibrations of the C=C-C=O unit. NMR analysis led to the conclusion that product 3a was the expected fused tetracyclic system where the 1,2-dihydrofuran ring was fused to the pinane and the cyclohexenone structural units. NMR spectra of 3a also confirmed that the obtained compound was a single diastereomer. Since this transformation started with enantiomerically pure substrate 1 whose configuration remains intact under the mild reaction conditions, the absolute configuration of the product 3a (Scheme 1) was determined from the 2D-NOESY experiment which showed a correlation between spatially close protons 9b-H ($\delta_{\rm H}$ 3.01), 4a-CH₃ ($\delta_{\rm H}$ 1.36) and 3-CH₃ ($\delta_{\rm H}$ 0.93 ppm), thereby establishing the stereochemistry as 2S,4R,4aR,9bR. The postulated absolute configuration of 3a conformed with the X-ray structure determined for the similar derivative **3d** (see below).

Next, we examined the [3+2] cyclization of ethyl nitroacetate **2b** with (1S)-(-)- α -pinene **1**. The reaction yielded exclusively a single enantiomer of isoxazole N-oxide **3b** as a methyl ester, which was due to transesterification with the solvent. We found, however, that this annulation could also be performed in ethanol or 2-propanol.

A replacement of methanol by higher alcohols allowed us to avoid the transesterification, providing enantiomerically pure iso-xazole N-oxide ethyl ester 3c (Scheme 1). In contrast to 3a and 3c which were oils, compound 3b was obtained in a crystalline form suitable for X-ray diffraction analysis. Isoxazole 3b crystallized in the non-centrosymmetric space group $P2_12_12_1$ and the crystal structure analysis confirmed the cyclization stereoselectivity. Since crystallization of 3b gave only small low quality needles, the absolute configuration was proved additionally with its reduced derivative 3d (Scheme 1) that gave better quality crystals. The molecular geometry observed in the crystal structure of 3b is shown in Fig. 1.

To rationalize the stereochemical outcome of the cyclization, we relied on the radical cyclization mechanism proposed by Lee et al. [9]. The key step determining the stereoselectivity is an attack of the nitroacetate C-radical on the α -pinene ring that may take place via path A or B (Scheme 2). Steric congestion imposed by the *gem*-dimethyl group (route A) favors addition from the less crowded side (route B). The produced tertiary radical **TR1** thus determines the absolute configuration at the newly formed stereogenic centre. After oxidation, **TR1** is transformed into a planar carbocation that undergoes nucleophilic attack with an oxygen atom of the nearby nitro group. This intramolecular ring closure leads to product **3** with two new contiguous stereogenic centers where the isoxazole ring must be *cis*-annulated because of steric reasons.

2.2. Cyclizations with norbornene and 1R-(-)-nopol

Norbornene (**4**), was another terpene-like olefin we explored for oxidative radical cyclization with ethyl nitroacetate. In the absence of stereogenic centers in the reactants, the cyclization, conducted in ethanol, gave racemic product **5**. Its detailed NMR analysis proved an *exo* configuration **5**, whereas no traces of an *endo* diastereoisomer were found (Scheme 3). When compared to α -pinene, norbornene revealed a reversal of the attack direction. In **4** the *exo* approach of nitroacetate was preferred because the methylene bridge offered less steric encumbrance than the ethylene unit on the *endo* side of the molecule. These results pointed out that steric hindrance, usually occurring in bridged bicyclic unsaturated rings, also strongly affects the stereochemistry of the oxidative radical cyclization process.

[3 + 2] annulation of ethyl nitroacetate with 1R-(-)-nopol (6) also demonstrated the role of the dimethylmethano group as a controlling element for the *endo* facial selectivity (Scheme 3). Previously we reported that CAN-mediated oxidative cyclizations can also be realized with unprotected alkenols [19]. Therefore, we used the chiral substrate **6** which upon cyclization with ethyl nitroacetate was converted to the isoxazole N-oxide derivative **7**. The synthesis was performed in ethanol to avoid transesterification. Similarly to (1S)-(-)- α -pinene **1**, cyclization of (1R)-(-)-nopol **6** took place in a highly stereospecific manner leading to enantiomerically pure product **7** (Scheme 3). The structure and configuration of **7** were determined by NMR spectroscopy including COSY, HSQC and NOESY experiments.

2.3. Cyclizations with (+)-camphene

To examine cyclizations with olefins having exocyclic methylene groups, we turned our attention to (+)-camphene **8** that offered the possibility of constructing a spiro-isoxazole motif. Treating enantiomerically pure **8** with ethyl nitroacetate in methanol gave rise to the expected heterocyclic compound **10** which, however, was a racemic mixture as established by chiral HPLC analysis. Racemisation of product **10** was also confirmed by X-ray crystal structure analysis. Compound **10** crystallized in the centrosymmetric

a: CAN/NaHCO₃ and dimedone in MeOH, RT; b: CAN/NaHCO₃ and ethyl nitroacetate in MeOH, RT; c: CAN/NaHCO₃ and ethyl nitroacetate in EtOH, RT; d: P(OEt)₃, 80⁰C, 30 h

Scheme 1. Diffunctionalization of (1S)-(-)- α -pinene with dimedone and ethyl nitroacetate promoted by CAN.

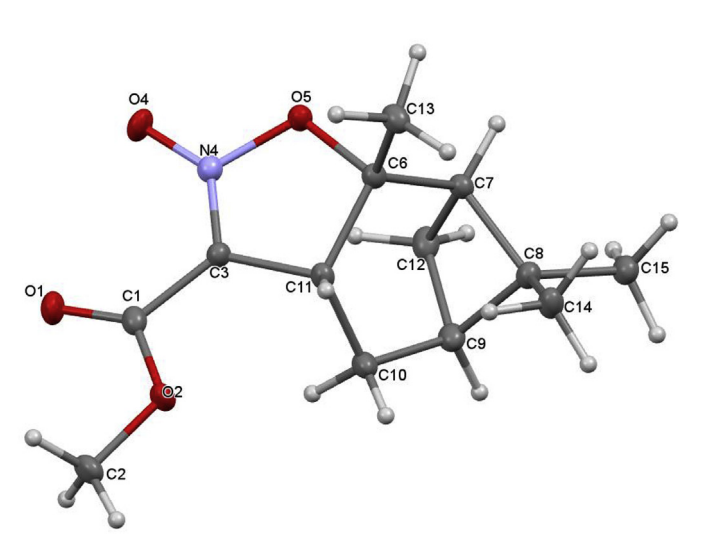
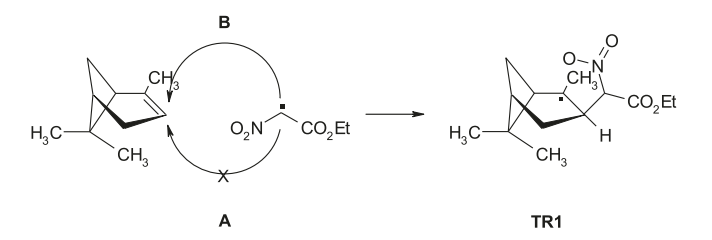


Fig. 1. X-ray crystal structure of **3b** (asymmetric unit) showing the atom labelling. The stereogenic centers at C6, C7 and C11 exhibit the R configuration. Displacement ellipsoids of non-hydrogen atoms are drawn at the 30% probability level. H atoms are presented as small spheres with an arbitrary radius.



Scheme 2. Stereochemical course of radical cyclization between (1*S*)-(-)- α -pinene and ethyl nitroacetate.

space group P^-1 , implying an equal amount of both enantiomers in the crystalline sample. According to the literature [20], we assume that the racemisation most likely proceeded via a mechanism involving non-classical carbocationic intermediates **9** produced by

one-electron oxidation of the radical adducts, as sketched in Scheme 4.

2.4. Cyclizations with R-(-)-carvone

R-(-)-carvone (11) represents an oxygenated chiral monoterpene for CAN-induced cyclizations with dimedone 2a and 2,4-pentanedione 2c. Both isolated products, which were dihydrofuran derivatives 12 and 13, were formed as equimolar mixtures of diastereoisomers, arising from the addition of the CH-acids to the more easily accessible exocyclic isopropenyl double bond (Scheme 5). The cyclization step was thought to proceed via an oxidized cationic intermediate (14), and hence was not stereoselective (Fig. 2)

According to previous studies and also our detailed analysis by electronic structure calculations (vide infra), the radical addition is exothermic and likely to take place via an early transition state reflecting the steric effects in the alkene reactant [21,22]. Since the transition state geometry resembles that of the reactants, structural features encountered in the substrate become crucial factor according to the Hammond postulate. This suggests that inherent steric hindrances present in the terpenoids play a key role in the stereochemical outcome of the oxidative radical cyclization.

2.5. Intramolecular cyclizations

Intramolecular cyclization of substrates comprising a C=C double bond and a tethered enolizable 1,3-dicarbonyl function represent interesting combinations with a potential for enhanced stereoselectivity. In this respect, the nopol hydroxyl group can be modified by etherification or esterification to provide an active methylene precursor for radical cyclization. Williamson etherification using chloroacetoacetate under mild conditions (NaH, THF) gave ether **15** which upon treatment with 2 mol of CAN in ethanol furnished two products in an approximately 2:1 ratio.

NMR spectra (1 H, 13 C, DEPT, and HSQC) of the major product **16** confirmed the presence of the 8-membered oxygen heterocycle that was fused to the carbocyclic scaffold. The lack of a methyl resonance from the *gem*-dimethyl moiety that was replaced by the signals for one terminal olefinic methylene ($\delta_{\rm H}$ 4.69, $\delta_{\rm C}$ 109.0) and one olefinic methine ($\delta_{\rm H}$ 5.70, $\delta_{\rm C}$ 127.2) suggested that the

Scheme 3. Oxidative cyclization of ethyl nitroacetate with bicyclic alkenes.

Scheme 4. Plausible mechanism for isomerization of (+)-camphene framework to racemic isocamphane derivatives through the non-classical carbocations.

Scheme 5. Regioselective cyclizations of CH-acids with *R*-(-)-carvone.

dimethylmethano bridge in the pinene moiety underwent a skeletal rearrangement, generating the isopropenyl group. The results of the NMR analysis allowed us to establish the benzo[d]oxocine-6carboxylate structure (**16**) for the major reaction product (Scheme

6).

The relative stereochemistry of **16** was determined by NOESY. The critical ¹H—¹H dipole-dipole interaction H-6 — H-6a was found to be only small, indicating there was no spatial proximity between

Fig. 2. Putative intermediate 14 in the [3+2] cyclization of dimedone and/or acety-lacetone with R-(-)-carvone.

them. Consequently, the oxocine methine H-6 and the bridgehead methine H-6a must be situated on the opposite faces of the 8-membered ring. In addition, the coupling constant of these protons, $J_{\text{H-6,H-6a}}\!=\!8.3\,\text{Hz}$, corresponded nicely to their anti arrangement.

As to the minor product 17, its 1 H and 13 C NMR spectra were essentially similar to those of 16, except for the loss of the = CH $_{2}$ resonance and the presence of additional signals for one methyl and one ethoxyl moiety. Taking into account these observations, the structure of 17 was readily established to be an ethyl ether derivative of 16 with an unchanged relative configuration (Scheme 6).

A plausible mechanism for the reaction shown in Scheme 6 can be envisioned as involving the generation of an electrophilic α,α' -dicarbonyl C-radical (**18**) at the active methylene group in **15**. Radical **18** selectively approaches the less hindered *endo* face of the pinene double bond while the adjacent ester group adopts an *exo* position (see below). Subsequent ring closure onto C=C double bond leads to a tertiary radical adduct (**19**) that undergoes homolytic β -fragmentation of the bridged *gem*-dimethylcyclobutane ring (\rightarrow **20**). The four-membered ring opening results in strain release and is accompanied by conformational change of the cyclohexene ring. The key acyclic radical intermediate **20** is oxidized forming **21** which is deprotonated to provide the benzoxazocine-6-carboxylate **16** (Scheme **7**). Alternatively, the cationic species **21** can be trapped by nucleophilic addition of ethanol giving **17**.

To further characterize the mechanism of the cyclization reactions, we carried out density functional theory (DFT) and ab initio calculations of structures and energies of several putative radical intermediates. The calculated transition state energies and partition functions were used for transition-state theory (TST) calculations of rate constants characterizing the relative reaction rates. The TST rate constants were least-squares fitted into Arrhenius parameters that were collated in Supplementary Table S22.

Oxidation of the starting ketoester was presumed to generate a transient C_{α} -radical to initiate the cyclization sequence. The C_{α} -radical can exist as isomers with a *syn* or an *anti*-alignment of the C=O groups, as represented by the respective structures *syn*-**18** and *anti*-**18** (Scheme 8).

Isomer *syn*-**18** was calculated to be 6.7 kJ mol⁻¹ more stable than *anti*-**18** (Table 1), indicating that the *syn* and *anti* isomers should be represented in a 56:44 ratio in an equilibrium mixture. These isomers can interconvert by a rotation about the ester $O = C - C_{\alpha}$ bond through a low-lying transition state (**TS**_{rot}, Scheme 8).

The calculated rate constant $(2.75 \times 10^8 \, \text{s}^{-1})$ at 298 K. Fig. 3) indicated a rapid interconversion of syn-18 and anti-18 under the reaction conditions. A transition state (TSrotb, Table S15, Supplementary Data) was also found for the rotation about the ketone O=C-C_{α} bond that had an energy (E(TS) = 28 kJ mol⁻¹) that was similar to that of \mathbf{TS}_{rot} , providing another pathway for rapid syn-anti isomerization of 18. In the next step, the C_{α} -radical can attack the pinene double bond to form the 8-membered heterocyclic ring in another radical intermediate (19, Scheme 8). To characterize this cyclization, we considered attacks at the endo and exo faces of the pinene double bond. In addition, the cyclization can proceed with the ketoester C_{α} -radical in the syn- and anti-carbonyl configurations and resulting in an exo or endo configuration of the ethoxycarbonyl substituent in 19. Scheme 8 illustrates ring closures via the syn-TS1 and anti-TS1 transition states of similar energies relative to syn-18, E(TS) = 31 and 32 kJ mol^{-1} , respectively. The corresponding TST rate constants, $syn-k_1 = 9.0 \times 10^6 \text{ s}^{-1}$ and anti $k_1 = 2.0 \times 10^6 \text{ s}^{-1}$, indicated fast cyclication preferring the synpathway. Note that cyclizations via both syn-TS1 and anti-TS1 proceeded from the endo-face of the pinene double bond and produced rotamers of intermediate 19a with an exo-configuration of the ethoxycarbonyl group. The cyclization was calculated to be 23 kJ mol⁻¹ exothermic (Table 1), indicating that a reverse opening of the 8-membered ring in 19a was disfavored. Intermediate 19a can undergo an exothermic cleavage of the pinene four-membered ring, forming the isopropyl radical intermediate 20 (Scheme 9) which was 43 kJ mol⁻¹ more stable than **19a** and 66 kJ mol⁻¹ more stable than syn-18 (Table 1).

The exothermicity of the consecutive cyclization and ring cleavage provided the driving force for the facile conversion of the C_{α} radical syn-18 to the bicyclic intermediate 20. The calculated kinetics for the reaction sequence converting syn-18 to 20 (eq. (1)) indicated negligible reverse ring opening in 19a (rate constant k_1) which was consumed by the fast forward reaction (rate constant k_2). The half-life for conversion of syn-18 to 20 was calculated as $t_{1/2} = 1.5$ ms at 298 K (Fig. 4), again indicating a fast overall conversion.

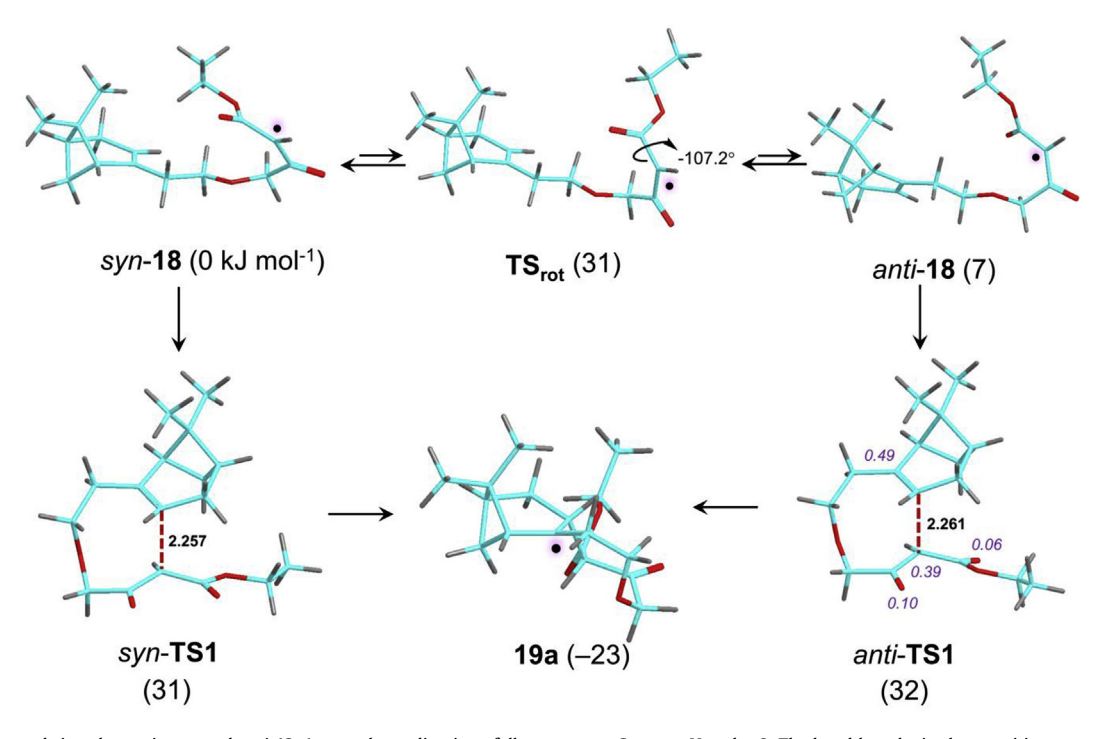
$$syn - 18 \xrightarrow{k_1} 19a \longrightarrow 20 \tag{1}$$

Cyclizations leading to the *endo*-facial, *endo*-COOC₂H₅ intermediate **19b** had transition states *syn*-**TS3** and *anti*-**TS3** (E(TS) = 39 and 34 kJ mol⁻¹, respectively, Table 1) that were at higher energies than those for *syn*-**TS1** and *anti*-**TS1**. As a consequence, the formation of **19b** (Scheme 10) was calculated to be ca. 20-fold slower that of **19a** (Fig. 3).

Likewise, the exo-facial cyclizations via *syn*-**TS4** and *anti*-**TS4** (Scheme 11) had still higher energies, E(TS) = 47 and 42 kJ mol^{-1} , respectively (Table 1), resulting in low rate constants for the formation of the cyclized intermediate **19c** (Fig. 3). Interestingly, intermediates **19b** and **19c** were thermodynamically more stable than **19a** (Table 1), and so the more facile formation of the latter isomer was entirely due to kinetic factors.

Scheme 6. Intramolecular oxidative radical cyclization of nopol derivative.

Scheme 7. Suggested mechanism leading to compounds 16 and 17.



Scheme 8. Rotation and ring closure in syn and anti-18. Atom color coding is as follows: cyan = C, gray = H, red = O. The bond lengths in the transition states are in Ångstrøms.

It should be noted that facile and exothermic cleavage of the cyclobutane ring $19a \rightarrow 20$ and the absence of the alternative cyclohexane ring opening was consistent with the ring strain enthalpies for hydrogenolysis of cycloalkanes (cyclohexane \rightarrow n-

hexane: 43.5 kJ mol^{-1} and cyclobutane \rightarrow butane: $153.2 \text{ kJ mol}^{-1}$) [23].

In order to verify the determined configuration of the bicyclic product **16**, which is an enantiopure compound, the theoretical

Table 1 Relative energies of radicals.

Species or reaction ^c	Relative Energy ^{a,b}			
	$\frac{\omega B97X-D}{6-31+G(d,p)}$	$\frac{\text{M06-2X}}{\text{6-31} + \text{G(d,p)}}$	M06-2X ^d 6-311++G(2d,p)	PMP2 ^{d,e} 6-311++G(2d,p)
anti-18	5	7	7 (7)	6
19a	-26	-24	-23 (-8)	-34
20	-63	-63	-66 (-58)	-74
19b	-29	-27	-26(-10)	-38
19c	-45	-41	-39 (-22)	-53
$syn-18 \rightarrow TS_{rot}$	32	31	31	31
$syn-18 \rightarrow syn-TS1$	27	30	31	21
syn- 18 → anti- TS1	30	32	32	22
$syn-18 \rightarrow TS2$	35	36	35	11
syn -18 $\rightarrow syn$ -TS3	36	38	39	27
$syn-18 \rightarrow anti-TS3$	32	33	34	24
syn- 18 → syn- TS4	45	45	47	36
syn- 18 → anti- TS4	42	40	42	32
19a → <i>syn</i> - TS1	53	54	53	55
19a → TS2	61	60	57	45
19b → <i>syn</i> - TS3	65	65	64	65

a In kJ mol⁻¹.

^f Relative free energies at 298 K in parentheses.

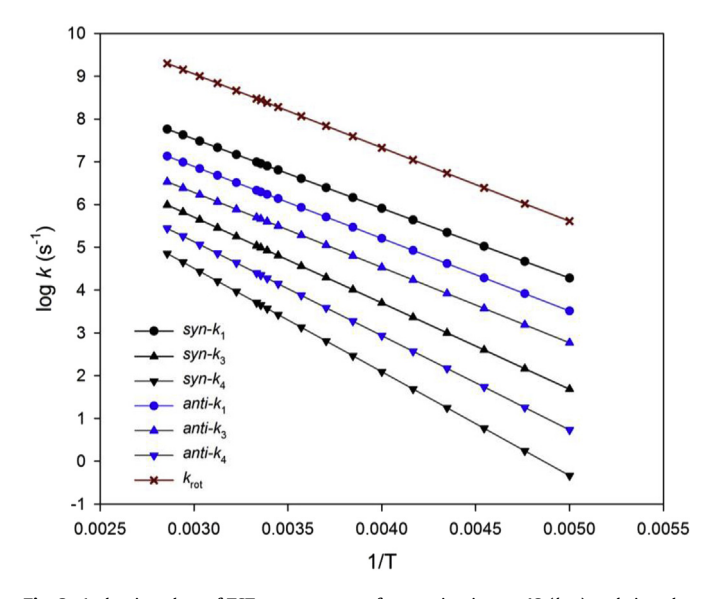


Fig. 3. Arrhenius plots of TST rate constants for rotation in syn-**18** (k_{rot}) and ring closures via syn-**TS1**, (syn- k_1), syn-**TS3**, (syn- k_3), syn-**TS4**, (syn- k_4), anti-**TS1**, (anti- k_1), anti-**TS3**, (anti- k_3), and anti-**TS4**, (anti- k_4).

electronic CD spectrum for the 6R,6aR,8R molecule was computed by time-dependent DFT with CAM-B3LYP-SCRF(acetonitrile)/6-311++G(d,p)//B3LYP/6-31G(d,p) (Fig. 5, left).

Comparison of the simulated spectrum with the recorded one (in MeCN) (Fig. 5, right) revealed a significant similarity between the experimental curve and the ECD trace for the "all-R" isomer. This correlation allowed us to corroborate the stereochemical structure of the heterocycle **16** as ethyl (6R,6aR,8R)-5-oxo-8-(prop1-en-2-yl)-1,4,5,6,6a,7,8,9-octahydro-2*H*-benzo[*d*]oxocine-6-carboxylate. In addition, since the experimental ECD spectra of the oxocine derivatives **16** and **17** closely resemble each other, we presume that both possess the same configuration, i.e. "all-R".

3. Conclusion

Oxidative cycloaddition of free radicals to chiral alkenes leads to the formation of products with new asymmetric centers. The highest stereoselectivity can be observed for addition to cyclic alkenes bearing endocyclic C=C double bonds. The stereoselectivity strongly depends on sterical hindrances and is especially efficient for chiral bicyclic alkenes, as oxidative cycloaddition to (1S)-(-)- α pinene gives only one diastereomer and the reaction is a fully stereospecific process. In contrast, in the absence of steric repulsion, the cycloaddition is non-stereoselective, furnishing mixtures of diastereoisomers. This was illustrated with the reaction of free radicals with enantiomerically pure R-(-)-carvone where oxidative cycloaddition involved the exocyclic C=C double bond forming an equimolar mixture of two diastereoisomers. Electronic structure calculations revealed that the radical attack on the endocyclic double bond had a low activation energy and resulted in an exothermic reaction. The calculated transition-state energies and rate constants were consistent with the observed stereospecificity.

4. Experimental

4.1. General

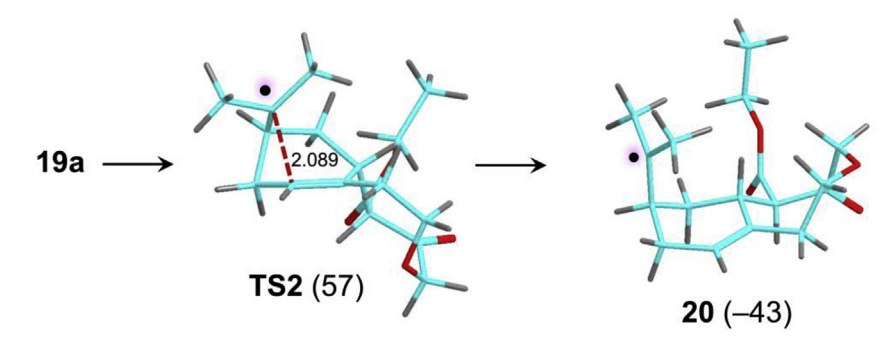
NMR spectra were determined on a Bruker Avance II 300 MHz and 600 MHz spectrometers (using TMS as an internal standard). IR spectra were measured on a Nicolet IR200 FT-IR spectrometer with a single-reflection ATR head. Microanalyses were carried out using CHNS Vario Micro Cube analyzer and their results were in good agreement with the calculated values. HPLC analysis was carried out on a Hitachi DAD equipped with a LiChroCART 250-4 column (heptane — isopropanol 9:1; 1.0 ml/min; monitored in the range 220—350 nm). Enantiomeric and diastereomeric ratios were determined using chiral HPLC chromatography on a Daicel Chiralpak AD-H column (hexane — isopropanol 9:1; 1 ml/min; monitored at 254 nm). Column chromatography was performed using commercial Merck silica gel 60 (230—400 mesh ASTM) and TLC

^b Including B3LYP/6-31+(d,p) zero-point vibrational energy corrections and referring to 0 K unless stated otherwise.

^c Including solvation energies by polarizable continuum model calculations in the ethanol dielectric.

^d From single point energy calculations on M06-2X/6-31 + G(d,p) optimized geometries.

^e Including energy corrections by annihilation of high spin states.



Scheme 9. Pinene ring cleavage in 19a. The relative energies (kJ mol⁻¹) and structure description are as in Scheme 8.

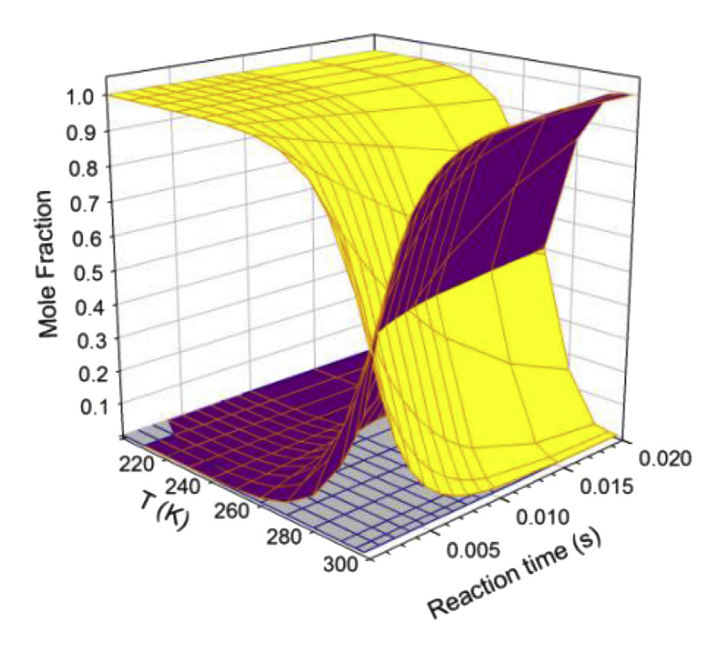


Fig. 4. Time and temperature dependence of molar fractions of syn-18 (yellow), 19a (gray), and 20 (magenta). Calculated from TST rate constants for syn-18 \rightarrow 19a (syn- k_1), 19a \rightarrow syn-18 (k_1), and 19a \rightarrow 20 (k_2) based on M06-2X/6-311++G(2d,p) TS energies.

analysis was carried out using Merck TLC silica gel 60 plates. Preparative thin-layer chromatography was performed with Chromatotron[®], model 7924T using glass rotor coated with 2 mm layer of Merck silica gel 60 PF254. Optical rotations were performed using a Jasco P-2000 polarimeter. Melting points were measured on an Electrothermal 9100 apparatus. X-ray diffraction data for single crystals of compounds 3b and its reduced derivatives 3d and 10 were collected using a SuperNova (Rigaku - Oxford Diffraction) four-circle diffractometer with a mirror monochromator and a microfocus CuK α radiation source ($\lambda = 1.54184\,\text{Å}$) which was applied for all single crystal diffraction experiments presented here. Additionally, the diffractometer was equipped with a CryoJet HT cryostat system (Oxford Instruments) allowing low temperature experiments, performed at 120(2) K for 3b, and 3d and 130(2) K for 10. The obtained data sets were processed with CrysAlisPro software [24]. The phase problem was solved with direct methods using SIR2004 [25]. The parameters of the obtained models were refined by full-matrix least-squares on F [2] using SHELXL-2014/6 [26]. Calculations were performed using WinGX integrated system (ver. 2014.1) [27]. Fig. 1 was prepared with Mercury 3.7 software [28].

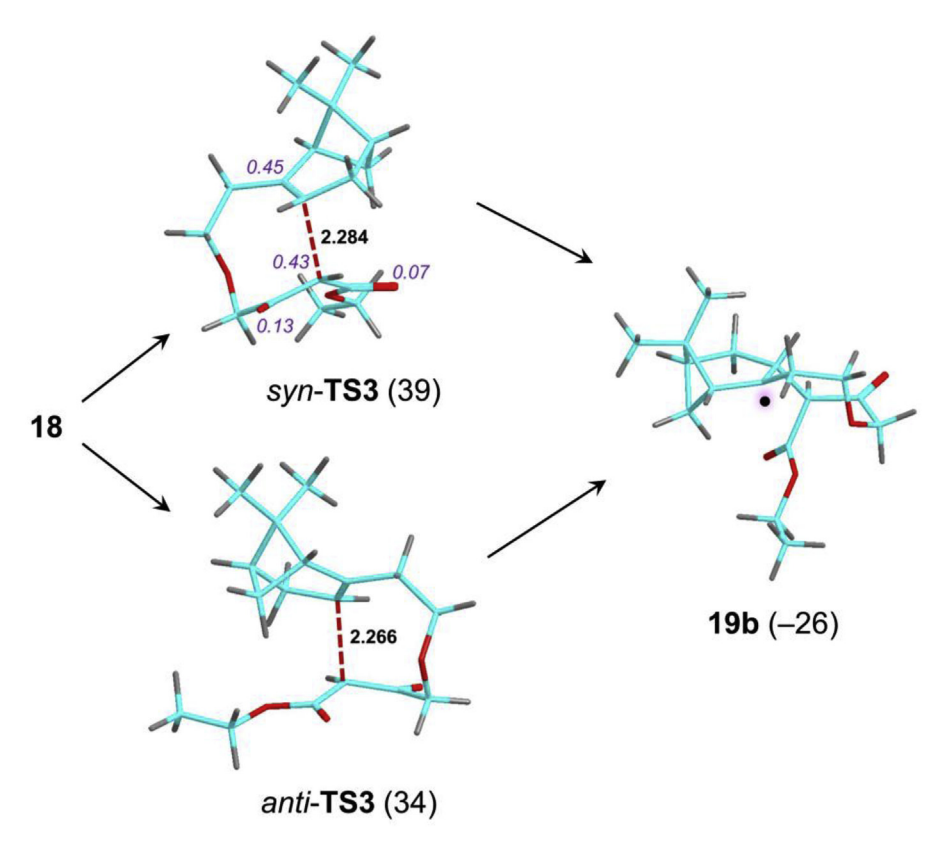
Crystallographic data have been deposited with the Cambridge Crystallographic Data Centre as supplementary publication nos.:

CCDC 1856133 (**3b**), CCDC 1856134 (**3d**) and CCDC 1856135 (**10**). Copies of the data can be obtained, free of charge, on application to CCDC, 12 Union Road, Cambridge CB2 1EZ, UK, (fax: +44-(0)1223-336033 or e-mail: deposit@ccdc.cam.ac.uk).

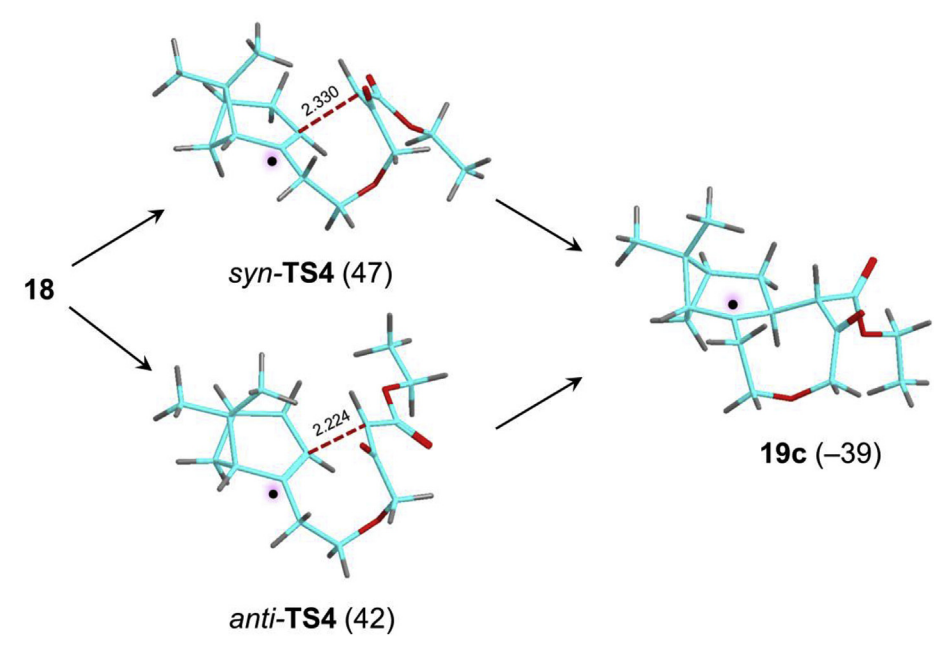
Calculations. All electronic structure calculations were performed with the Gaussian 09 (Revision A.02) program package [29]. Radical structures were obtained at several levels of theory, starting with conformer analysis and followed by full gradient geometry optimization, transition state search, and intrinsic reaction coordinate analysis [30]. Initial structures were obtained by density functional theory (DFT) calculations in a spin-unrestricted formalism using the B3LYP [31] hybrid functional with the 6-31 + G(d.p) basis set. The fully optimized gas-phase structures were used as initial guesses for ωB97X-D [32], and M06-2X [33] geometry optimizations with the 6-31 + G(d,p) basis set. These geometry optimizations included solvation energies in the ethanol dielectric obtained with the polarizable continuum model [34] using standard parameters from Gaussian 09. The structures were confirmed as local energy minima or first-order saddle points (transition states) by harmonic frequency analysis giving the appropriate number (0 and 1, respectively) of imaginary frequencies. The optimized structures, total energies, and zero-point vibrational energies of major species are given in the Supplement. Relative and transition-state energies were based on single-point energy calculations with DFT and Møller-Plesset [35] (UMP2, frozen core) methods using the 6-311++G(2d,p) basis set. Higher spin states in UMP2 energies were annihilated by spin projection [36,37], providing spin expectation values of <0.78 for local energy minima and <0.9 for transition states. Atomic charge and spin densities were obtained with Natural Population Analysis [38] of the M06-2X/6-311++G(2d,p) wave functions.

4.2. General procedure for oxidative cycloaddition of CH-acids to alkenes

2.55 mmol of CH-acid and 2.55 mmol of a desired alkene were solved in methanol or ethanol (30 ml) in a 100 mL conical flask. The flask was filled with argon, placed on a magnetic stirrer in the icebath and the reaction mixture was cooled below 5 °C. Next sodium bicarbonate (0.536 g, 6.38 mmol, 1.5 eq) and ceric ammonium nitrate (3.5 g, 6.38 mmol, 1.5 eq) were added and the reactants were stirred and the reaction was monitored using TLC method (silica gel TLC plates, CHCl₃—MeOH 30:1). After the oxidative cycloaddition was completed, the solvent was evaporated under vacuum and products were extracted with CHCl₃ (3x30 mL). The combined extracts were evaporated to dryness and the crude products were submitted to flash chromatography (SiO₂, CHCl₃—MeOH 20:1). Finally, the chromatotrone was used to obtain the pure adducts (SiO₂/gypsum, eluent: CHCl₃—MeOH 30:1).



Scheme 10. Alternative endo-facial ring closure in syn and anti-18. The relative energies (kJ mol⁻¹) and structure description are as in Scheme 8.



Scheme 11. Exo-facial ring closure in syn and anti-18. The relative energies (kJ mol⁻¹) and structure description are as in Scheme 8.

4.2.1. (2S,4R,4aR,9bR)-3,3,4a,7,7-pentamethyl-2,3,4,4a,6,7,8,9b-octahydro-2,4-methanodibenzo[b,d]furan-9(1H)-one (**3a**)

Isolated yield 0.335 g (48%); colorless oil, $[\alpha]_D^{25} = -75.8$ (c = 0.14, CH₃CN); IR: $\nu_{\rm max}$ 2943, 2918, 2861, 1617, 1393, 1362, 1276, 1235, 1203, 1166, 1142, 1118, 1087, 1029, 1010 cm⁻¹; ¹H NMR (CDCl₃) δ 0.92 (s, 3H, 3-Me), 0.97 (d, 1H, J = 10.5 Hz, 10H α), 1.09 (s, 3H, 7-Me), 1.11

(s, 3H, 7-Me), 1.28 (s, 3H, 3-Me), 1.36 (s, 3H, 4a-Me), 1.70 (ddd, 1H, J = 13.8, 3.4 Hz, 1-Ha), 1.88-1.93 (m, 1H, 4-H), 2.13 (dd, 1H, J = 10.5, 4.9 Hz, 10-Hb), 2.15-2,18 (m, 1H, 2-H), 2.20 (m, 2H, 6-H), 2.23 (m, 2H, 8-H), 2.27-2.33 (m, 1H, 1-Hb), 3.01 (m, 1H, 4b-H); 13 C NMR (CDCl₃) δ 22.9, 26.2, 27.1, 27.4, 27.9, 29.2, 32.4, 34.0, 37.9, 37.9, 38.2, 39.4, 50.6, 51.0, 97.6, 118.6, 174.0, 194.8; Anal. Calcd for $C_{18}H_{26}O_4$

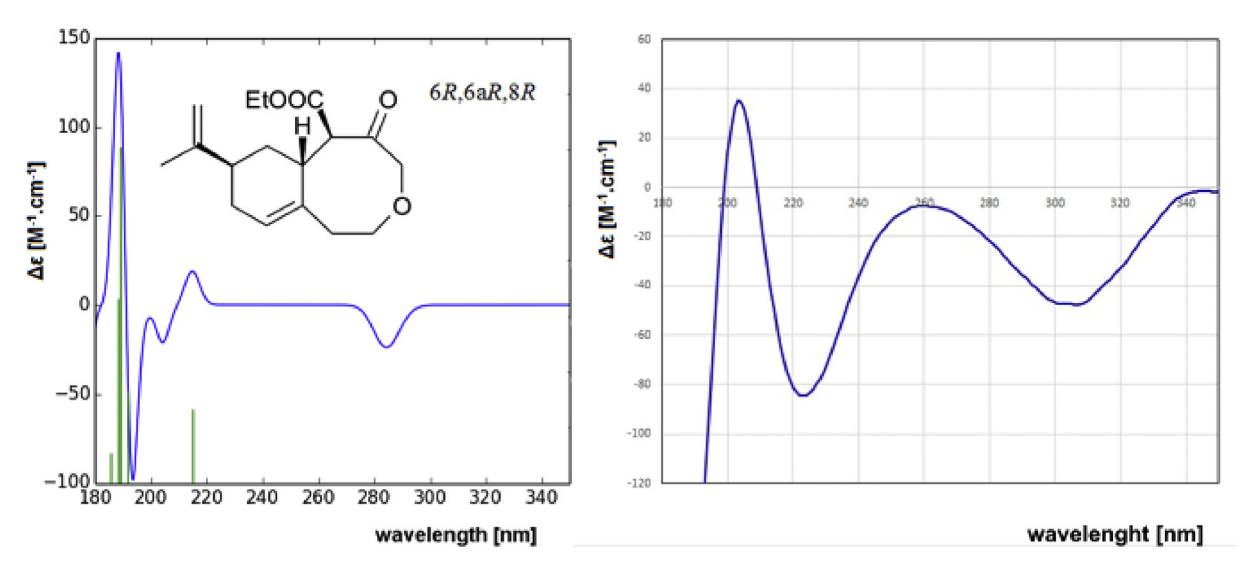


Fig. 5. Calculated (left) and experimental (right) CD spectra of 16.

(274.41): C, 78.79; H, 9.55%. Found C, 78.88; H, 9.74%.

4.2.2. (3aR,5R,7R,7aR)-3-(methoxycarbonyl)-6,6,7a-trimethyl-3a,4,5,6,7,7a-hexahydro-5,7-methanobenzo[d]isoxazole-2-oxide (3b)

Isolated yield 0.355 g (55%); colorless fine solid; mp 43 °C; $[\alpha]_D^{25}=+35.8$ (c=0.14, CH₃CN); IR: $\nu_{\rm max}$ 2971, 1735, 1698, 1606, 1563, 1440, 1378, 1290, 1272, 1242, 1194, 1147, 1000 cm⁻¹; ¹H NMR (CDCl₃) δ 0.94 (s, 3H, 6-Me), 1.31 (s, 3H, 6-Me), 1.34 (m, 1H, 8-Ha), 1.50 (s, 3H, 7a-Me), 1.84 (ddd, 1H, J=7.2, 3.2, 4.2 Hz, 4-Ha), 2.03 (m, 1H, 5-H), 2.11 (dd, 1H, J=9.3, 4.9 Hz, 4-Hb), 2.35 (m, 2H, 7-H and 8-Hb), 3.50 (m, 1H, 3a-H), 3.87 (s, 3H, OMe); ¹³C NMR (CDCl₃) δ 23.1, 26.8, 27.0, 27.3, 32.5, 38.2, 38.8, 41.8, 49.2, 52.4, 86.4, 114.4, 159.9; Anal. Calcd for C₁₃H₁₉NO₄ (253.30): C, 61.64; H, 7.56; N, 5.53%. Found C, 61.73; H, 7.82; N 5.58%.

4.2.3. (3aR,5R,7R,7aR)-3-(ethoxycarbonyl)-6,6,7a-trimethyl-3a,4,5,6,7,7a-hexahydro-5,7-methanobenzo[d]isoxazole-2-oxide (**3c**)

Isolated yield 0.41 g (60%); colorless oil; $[\alpha]_D^{25} = +26.4$ (c=0.12; CH₃CN); IR: $\nu_{\rm max}$ 2927, 1733, 1696, 1608, 1561, 1450, 1380, 1273, 1241, 1179, 1020 cm⁻¹; $^1{\rm H}$ NMR (CDCl₃) δ 0.94 (s, 3H, 6-Me), 1.25–1.30 (m, 1H, 8-Ha), 1.31 (s, 3H, 6-Me), 1.34 (t, 3H, J=7.1 Hz, OCH₂Me), 1.50 (s, 3H, 7a-Me), 1.84 (ddd, 1H, J=7.2, 3.2, 4.2 Hz, 4-Ha), 2.02 (m, 1H, 5-H), 2.11 (m, 1H, 4-Hb), 2.35 (m, 2H, 7-H and 8-Hb), 3.49 (m, 1H, 3a-H), 4.30 (dq, 1H, J=10.9, 7.1 Hz, OCHaHb), 4.35 (dq, 1H, J=10.9, 7.1 Hz, OCHaHb); $^{13}{\rm C}$ NMR (CDCl₃) δ 14.2, 23.1, 26.8, 27.0, 27.3, 32.5, 38.2, 38.8, 41.8, 49.2, 61.6, 86.2, 114.4, 159.3; Anal. Calcd for C₁₄H₂₁NO₄ (267.33): C, 62.90; H, 7.92; N 5.24%. Found C, 62.76; H, 7.88; N, 5.34%.

4.2.4. Methyl (3aR,5R,7R,7aR)-6,6,7a-trimethyl-3a,4,5,6,7,7a-hexahydro-5,7-methanobenzo[d]isoxazole-3-carboxylate (**3d**)

Isolated yield 0.39 g (64%); colorless fine crystals, mp 78 °C; $[\alpha]_D^{25}=+29.7$ (c = 0.11; CH₃CN); IR: $\nu_{\rm max}$ 2924, 1716, 1582, 1443, 1372, 1268, 1248, 1208, 1141, 1112, 963, 947, 794 cm $^{-1}$; 1 H NMR (CDCl₃) δ 0.93 (s, 3H, 6-Me), 1.31 (s, 3H, 6-Me), 1.34 (m, 1H, 8-Ha), 1.40 (s, 3H, 7a-Me), 1.75 (ddd, 1H, J=7.2, 3.2, 4.2 Hz, 4-Ha), 1.97 (m, 1H, 5-H), 2.18 (dd, 1H, J=4.9, 6.0 Hz, 4-Hb), 2.30 (m, 2H, 7-H and 8-Hb), 3.25 (dd, 1H, J=10.8, 4.0 Hz, 3a-H), 3.89 (s, 3H, OMe); 13 C NMR (CDCl₃) δ 23.0, 26.4, 26.8, 26.9, 30.3, 37.8, 39.0, 43.9, 49.6, 52.5, 95.4, 154.5, 161.5; Anal. Calcd for C₁₃H₁₉NO₃ (237.30): C, 65.80; H, 8.07; N,

5.90%. Found: C, 65.51; H, 8.09; N 5.73%.

4.2.5. 3-(ethoxycarbonyl)-3a,4,5,6,7,7a-hexahydro-4,7-methanobenzo[d]isoxazole-2-oxide (5)

Isolated yield 0.37 g (65%); yellowish oil; IR: $\nu_{\rm max}$ 2952, 1724, 1613, 1553, 1372, 1238, 1171, 1090, 1024, 855, 735 cm⁻¹; $^{1}{\rm H}$ NMR (CDCl₃) δ 1.15 (m, 1H, 5-Ha), 1.27 (m, 1H, 6-Ha), 1.33 (t, 3H, J = 8.3 Hz, OCH₂Me), 1.34 (dt, 1H, J = 11.1 Hz, 8-Ha), 1.59 (m, 1H, 6-Hb), 1.62 (m, 1H, 5-Hb), 1.72 (dt, 1H, J = 11.1 Hz, 8-Hb), 2.56 (m, 2H, 4-H and 7-H), 3.46 (dd, 1H, J = 8.3, 1.3 Hz, 3a-H), 4.31 (ddq, 2H, J = 9.1, 7.1 Hz, OCH₂), 4.55 (dt, 1H, J = 8.3, 1.1 Hz, 7a-H); I NMR (CDCl₃) δ 14.1, 22.7, 27.2, 32.4, 40.4, 42.1, 52.6, 61.6, 81.1, 109.6, 159.2; Anal. Calcd for C₁₁H₁₅NO₄ (225.25): C, 58.66; H, 6.71; N, 6.22%. Found: C, 58.73; H, 6.54; N, 6.10%.

4.2.6. (3aR,5R,7R,7aR)-3-(ethoxycarbonyl)-7a-(2-hydroxyethyl)-6,6-dimethyl-3a,4,5,6,7,7a-hexahydro-5,7-methanobenzo[d] isoxazole-2-oxide (7)

Isolated yield 0.36 g (48%); colorless solid; mp 82-84 °C; $[\alpha]_D^{25}=+20.9$ (c = 0.11, CH₃CN); IR: $\nu_{\rm max}$ 3489, 2910, 2862, 1706, 1585, 1374, 1244, 1182, 1051, 1011, 876, 803, 581 cm $^{-1}$; 1 H NMR (CDCl₃) δ 0.94 (s, 3H, 6-Me), 1.31 (s, 3H, 6-Me), 1.31 (d, 1H, J= 11.0 Hz, 8-H), 1.34 (t, 3H, J= 7.1 Hz, OCH₂Me), 1.69 (br s, 1H, OH), 1.86 (m, 1H, 7a-CHa), 1.94 (dt, 1H, J= 14.8, 5.9 Hz, 4-H), 2.03 (m, 1H, 5-H), 2.16 (dt, 1H, J= 14.8, 5.9 Hz, 4-H), 2.27 (dd, 1H, J= 4.9, 5.1 Hz, 7-H), 2.36 (m, 2H, 7a-CHb and 6-H), 3.70 (m, 1H, 3a-H), 3.79—3.89 (m, 2H, CH₂—OH), 4.27—4.38 (ddq, 2H, J= 10.9, 7.1 Hz, COO—CH₂); 13 C NMR (CDCl₃) δ 14.2, 23.2, 26.3, 27.0, 32.6, 38.2, 38.9, 41.0, 42.4, 47.5, 58.1, 61.7, 87.4, 114.9, 159.2; Anal. Calcd for C₁₅H₂₃NO₅ (297.35); C, 60.59; H, 7.80; N, 4.71%. Found: C, 60.65; H, 7.91; N, 4.85%.

4.2.7. (1S,2R,4R)-3'-(methoxycarbonyl)-3,3-dimethyl-4H-spiro [bicyclo[2,2,1]heptane-2,5'-isoxazole]-2'-oxide (**10a**) and (1R,2S,4S)-3'-(methoxycarbonyl)-3,3-dimethyl-4H-spiro[bicyclo [2,2,1]heptane-2,5'-isoxazole]-2'-oxide (**10b**)

Isolated yield 0.47 g (73%); colorless crystals; mp 52-53 °C; $[\alpha]_D^{25}$ = 0.0 (c = 0.1, CH₃CN); IR: $\nu_{\rm max}$ 2957, 2880, 1727, 1608, 1462, 1255, 1157, 1030, 868, 798, 721, 611 cm⁻¹; ¹H NMR (CDCl₃) δ 1.00 (s, 3H, 3-Me), 1.07 (s, 3H, 3-Me), 1.25 (m, 2H, 5-H), 1.32 (m, 1H, 7-Ha), 1.53–1.57 (m, 2H, 6-H), 1.85 (m, 1H, 4-H), 1.86 (d, 1H, J = 10.5 Hz, 7-Hb), 2.36 (m, 1H, 1-H), 3.21 (d, 1H, J = 17.2 Hz, 4'-Ha), 3.28 (d, 1H,

J = 17.2 Hz, 4'-Hb), 3.85 (s, 3H, OMe); ¹³C NMR (CDCl₃) δ 21.5, 23.8, 24.6, 24.6, 32.5, 35.0, 44.1, 47.3, 48.6, 52.5, 92.9, 109.7, 159.8; Anal. Calcd for C₁₃H₁₉NO₄ (253.30): C, 61.64; H, 7.36; N, 5.53%. Found: C, 61.58; H, 7.45; N, 5.43%.

4.2.8. (S)-2,6,6-Trimethyl-2-((R)-4-methyl-5-oxocyclohex-3-en-1-yl)-3,5,6,7-tetrahydrobenzofuran-4(2H)-one and (R)-2,6,6-trimethyl-2-((R)-4-methyl-5-oxocyclohex-3-en-1-yl)-3,5,6,7-tetrahydrobenzofuran-4(2H)-one ($\mathbf{12}$)

Isolated yield 0.48 g (65%); colorless oil; IR: $\nu_{\rm max}$ 2959, 2923, 1672, 1614, 1403, 1354, 1242, 1217, 1032, 1018, 634 cm⁻¹; ¹H NMR (CDCl₃) δ 1.07 and 1.08 (s, 3H, 6-Me), 1.10 (s, 3H, 6-Me), 1.38 and 1.39 (s, 3H, 2-Me), 1.77 (br s, 3H, =C-Me), 2.17 (m, 1H, 1-H), 2.20 and 2.21 (br.s, 2H, 7-H), 2.25 (br.s, 2H, 5-H), 2.27-2.58 (m, 5H), 2.77 and 2.80 (dt, 1H, J = 14.6 Hz, 3-Ha), 6.71 and 6.73 (m, 1H, =CH); ¹³C NMR (CDCl₃) δ 15.6, 24.5 and 24.9, 26.7, 28.4 and 28.5, 28.8, 34.1, 34.6 and 35.2, 37.8, 38.6 and 38.7, 44.1 and 44.2, 50.8, 93.2, 110.9, 135.6, 143.8, 174.8 and 174.9, 194.7 and 194.8, 198.6 and 198.7; Anal. Calcd for C₁₈H₂₄O₃ (288.39): C, 74.97; H, 8.39%. Found: C,75.15; H 8.24%.

4.2.9. (R)-5-((S)-4-acetyl-2,5-dimethyl-2,3-dihydrofuran-2-yl)-2-methylcyclohex-2-en-1-on and (R)-5-((R)-4-acetyl-2,5-dimethyl-2,3-dihydrofuran-2-yl)-2-methylcyclohex-2-en-1-on (13)

Isolated yield 0.35 g (65%); colorless oil; IR: $\nu_{\rm max}$ 2080, 1712, 1673, 1447, 1382, 1226, 1144, 1095, 1063, 974 cm⁻¹; ¹H NMR (CDCl₃) δ 1.33 and 1.34 (s, 3H, 2-Me), 1.77 and 1.78 (d, 3H, ⁴J = 1.3 Hz, =C-Me), 2.15 (m, 1H, 5-H), 2.19 (br.s, 6H, 2Me), 2.24, (m, 1H, 4-Ha), 2.27 (m, 1H, 4-Hb), 2.36 (m, 1H, 6-Ha), 2.48-2.54 (m, 1H, 6-Hb), 2.57-2.62 (dt, 1H, J = 14.4 Hz, 3-Ha), 2.87-2.93 (dt, 1H, J = 14.4 Hz, 3-Hb), 6.73 (m, 1H, =CH); ¹³C NMR (CDCl₃) δ 15.0 and 15.1, 15.6, 24.4 and 24.5, 26.7, 29.3, 38.7 and 38.8, 39.5 and 39.7, 44.1 and 44.2, 88.5, 111.7 and 111.8, 135.54, 144.0, 166.3, 194.3, 198.8 and 198.96; Anal. Calcd for C₁₅H₂₀O₃ (248.32): C, 72.55; H, 8.12%. Found: C, 72.24; H 8.25%.

4.3. Synthesis of ethyl 4-(2-((1R,5R)-6,6-dimethylbicyclo[3.1.1] hept-2-en-2-yl)ethoxy)-3-oxobutanoate (15)

(1*R*)-(-)-nopol (5 ml, 31.1 mmol), sodium hydride (60% dispersion in mineral oil, 2.5 g, 62.2 mmol) and 25 ml of anhydrous diethyl ether were placed in 50 ml round bottomed flask and stirred under argon at room temperature for 1.5 h. Then fresh destilated ethyl 4-chloro3-oxobutanolate (4.2 ml, 31.1 mmol) was added and stirring was continued under argon atmosphere for another 48 h. After this time the reaction was terminated by addition of 5 ml of water and the solvent was evaporated to near dryness. The crude product was suspendered in 25 ml of water and acidified to pH 5 using 98% sulphuric acid. The obtained mixture was extracted 3 times with 50 ml of diethyl ether and combined organic extracts were dried over MgSO₄ and evaporated furnishing the crude product 15. Purification through the column chromatography (silica gel, eluent: pentane-ethyl acetate 7:1) led to 1.63 g of pure product 15.

Isolated yield 1.63 g (18%); yellowish oil; $[\alpha]_D^{25} = -28.0$ (c = 0.18; CH₃CN); IR: $\nu_{\rm max}$ 2974, 2904, 2824, 1722, 1651, 1314, 1223, 1113, 1034; $^1{\rm H}$ NMR (CDCl₃) δ 0.81 (s, 3H, 6-Me), 1.14 (d, 1H, J = 8.5 Hz, 7-Ha), 1.26 (s. 3H, 6-Me), 1.27 (t, 3H, J = 7.1 Hz, OCH₂Me), 2.00–2.10 (m, 2H, 1-H and 5-H), 2.20–2.40 (m, 5H, 7-Hb, =C—CH₂, 4-Ha, 4-Hb), 3.49 (t, 2H, J = 7.0 Hz, OCH₂), 3.51 (s, 2H, COCH₂CO₂), 4.07 (s, 2H, OCH₂CO), 4.18 (q, 2H, J = 7.1 Hz, COOCH₂), 5.27 (m, 1H, =CH); $^{13}{\rm C}$ NMR (CDCl₃) δ 14.0, 21.1, 26.2, 31.3, 31.6, 36.9, 37.9, 40.7, 45.8, 45.9, 61.3, 70.2, 75.6, 118.3, 144.5, 167.0, 202.2; Anal. Calcd for C₁₇H₂₆O₄ (294.39): C, 69.36; H, 8.90%. Found: C, 69.47; H, 9.02%.

4.4. Synthesis of ethyl (6R,6aR,8R)-5-oxo-8-(prop-1-en-2-yl)-1,4,5,6,6a,7,8,9-octahydro-2H-benzo[d]oxocine-6-carboxylate (16) and ethyl (6R,6aR,8R)- 8-(2-ethoxypropan-2-yl)- 5-oxo-1,4,5,6,6a,7,8,9-octahydro-2H-benzo[d]oxocine-6-carboxylate (17)

Ethyl 4-(2-((1R,5R)-6,6-dimethylbicyclo[3.1.1]hept-2-en-2-yl) ethoxy)-3-oxobutanoate (15) (0.442 g, 1.5 mmol), sodium bicarbonate (0.315 g, 3.75 mmol), cerium ammonium nitrate (2.05 g, 3.75 mmol) and 30 ml of anhydrous EtOH were placed in 100 ml conical flask filled with argon and fitted wit CaCl₂ tube. Reaction mixture was stirred at room temperature overnight. After this time the solvent was evaporated to dryness. The crude product was submitted to flash chromatography (SiO₂, eluent: pentane-AcOEt, 2:1) and pure main product 16 and by-product 17 were isolated using centrifugal thin-layer chromatograph (Merck silica gel 60 PF254, eluent: pentane-AcOEt 7:1).

4.4.1. Ethyl (6R,6aR,8R)-5-oxo-8-(prop-1-en-2-yl)-1,4,5,6,6a,7,8,9-octahydro-2H-benzo[d]oxocine-6-carboxylate (16)

Isolated yield 80 mg (15%); colorless oil; $\alpha_D^{25} = -77.8$ (c = 0.15; CH₃CN); IR: ν_{max} 2912, 1739, 1703, 1444, 1364, 1240, 1171, 1086, 1025, 887 cm⁻¹; ¹H NMR (CDCl₃) δ 1.24 (t, 3H, J = 7.1 Hz, OCH₂Me), 1.71 (s, 3H, Me), 1.71 (ddd, 1H, J = 13.6, 5.6 Hz, 7-Ha), 1.80 (ddd, 1H, J = 13.6 Hz, 7-Hb), 1.96 (ddd, 1H, J = 10.5 Hz, 9-Ha), 2.10 (m, 1H, 1-Ha), 2.16 (m, 1H, 9-Hb), 2.27 (m, 1H, 1-Hb), 2.28 (m, 1H, 8-H), 3.00 (m, 1H, 6a-H), 3.66 (ddd, 1H, J = 12.0, 3.9 Hz, 2-Ha), 3.85 (ddd, 1H, J = 12.0, 4.9, 1.9 Hz, 2-Hb), 3.92 (d, 1H, J = 8.2 Hz, 6-H), 3.97 (d, 1H, J = 17.0 Hz, 4-Ha), 4.02 (d, 1H, J = 17.0 Hz, 4-Hb), 4.18 (m, 2H, COOCH₂), 4.67 (d, 1H, J = 22.2 Hz, =CHaHb), 4.74 (d, 1H, J = 22.2 Hz, =CHaHb), 5.71 (m, 1H, =CH); ¹³C NMR (CDCl₃) δ 14.0, 20.7, 30.9, 34.1, 35.6, 35.8, 41.7, 60.7, 61.2, 75.6, 77.4, 109.0, 127.1, 135.4, 148.8, 168.6, 210.3; Anal. Calcd for C₁₇H₂₄O₄ (292.37): C, 69.84; H, 8.27%. Found: C, 69.94; H, 8.40%.

4.4.2. Ethyl (6R,6aR,8R)- 8-(2-ethoxypropan-2-yl)- 5-oxo-1,4,5,6,6a,7,8,9-octahydro-2H-benzo[d]oxocine-6-carboxylate (17)

Isolated yield 45 mg (8%); colorless oil; $[\alpha]_D^{25} = -126.8$ (c = 0.15; CH₃CN); IR: ν_{max} 2912, 1739, 1703, 1444, 1240, 1199, 1171, 1086, 1025, 887, 518; ^1H NMR (CDCl₃) δ 1.07 (s, 6H, 2Me), 1.11 (t, 3H, J = 6.9 Hz, OCH₂Me), 1.24 (t, 3H, J = 7.1 Hz, OCH₂Me), 1.48 (m, 1H, 7-Ha), 1.80–1.92 (m, 3H, 1-Ha, 9-Ha and 8-H), 2.05 (m, 2H, 7-Hb, 9-Hb), 2.26 (m, 1H, 1-Hb), 2.97 (m, 1H, 6a-H), 3.36 (ddq. 2H, J = 14.0, 8.7, 6.9 Hz, OCH₂), 3.64 (ddd, 1H, J = 11.5, 8.2, 4.0 Hz, 2-Ha), 3.82 (ddd, 1H, J = 11.5, 8.2, 5.0 Hz, 2-Hb), 3.90 (d, 1H, J = 8.35 Hz, 6-H), 3.98 (dd, 2H, J = 16.9 Hz, 4-H), 4.17 (ddq, 2H, J = 17.3, 7.2, 4.7 Hz, OCH₂), 5.69 (br s, 1H, =CH); 13 C NMR (CDCl₃) δ 14.0, 16.1, 22.7, 27.3, 30.2, 35.5, 36.4, 42.2, 55.9, 60.7, 61.2, 75.7, 75.8, 127.5, 135.4, 168.7, 210.4; Anal. Calcd for C₁₉H₃₀O₅ (338.45): C, 67.43; H, 8.93%. Found: C, 67.58; H, 8.85%.

Acknowledgments

This work was supported by the Grant Agency of the Slovak Republic (VEGA 1/0262/19). Research at the University of Washington was supported by the Chemistry Division of the U.S. National Science Foundation (Grants CHE-1661815 and CHE-1624430). F.T. thanks the Klaus and Mary Ann Saegebarth Endowment for general support. The research was carried out with the equipment purchased thanks to the financial support of the European Regional Development Fund in the framework of the Polish Innovation Economy Operational Program (Contract No. POIG.02.01.00-12-023/08).

Appendix A. Supplementary data

Supplementary data to this article can be found online at https://doi.org/10.1016/j.tet.2019.03.039.

References

- [1] (a) E.I. Heiba, R.M. Dessau, J. Am. Chem. Soc. 93 (1971) 995;
 - (b) E.I. Hevba, R.M. Dessau, P.G. Rodewald, I. Am. Chem. Soc. 96 (1974) 7977.
- (a) M.E. Kurz, P. Ngoviwatchai, J. Org. Chem. 46 (1981) 4672; (b) M.E. Kurz, V. Baru, P.N. Nguyen, J. Org. Chem. 49 (1984) 1603.
- [3] E. Baciocchi, R. Ruzziconi, J. Org. Chem. 51 (1986) 1645.
- [4] E. Baciocchi, R. Ruzziconi, Synth. Commun. 18 (1988) 1841.
- [5] E. Baciocchi, G. Civatarese, R. Ruzziconi, Tetrahedron Lett, 28 (1987) 5357.
- [6] V. Nair, J. Mathew, J. Chem. Soc. Perkin Trans. 1 (1985) 187.
- [7] S. Maiti, P.T. Perumal, J.C. Menéndez, Tetrahedron 66 (2010) 9512.
- [8] G. Savitha, S.K. Niveditha, D. Muralidharan, P.T. Perumal, Tetrahedron Lett. 48 (2007) 2943.
- [9] YR Lee BS Kim DH Kim Tetrahedron 56 (2000) 8845
- [10] A. D'Annibale, A. Pesce, S. Resta, C. Trogolo, Tetrahedron Lett. 38 (1997) 1829.
- [11] A.-I. Tsai, C.-P. Chuang, Tetrahedron 62 (2006) 2235.
- [12] E. Elamparuthi, B.G. Kim, J. Yin, M. Maurer, T. Linker, Tetrahedron 64 (2008) 11925.
- [13] A.-C. Durand, E. Dumez, J. Rodriguez, J.-P. Dulcère, Chem. Commun. (1999) 2437
- [14] V. Nair, L.G. Nair, L. Balagopal, J. Mathew, Indian J. Chem., Sect. B 39B (2000) 352
- [15] (a) M.L. Wise, R. Croteau, in: D. Sir Barton, K. Nakanishi, O. Meth-Cohn (Eds.), Comprehensive Natural Products Chemistry, vol. 2, Elsevier Science, Oxford, 1999, pp. [97]-[154];
 - (b) E. Breitmaier, Terpenes: Flavors, Fragrances, Pharmaca, Pheromones, Wiley- VCH Verlag, Weinheim, 2006.
- [16] Z.G. Brill, M.L. Condakes, C.P. Ting, T.J. Maimone, Chem. Rev. 117 (2017) 11753.
- [17] (a) K.S. Cho, Y. Lim, K. Lee, J. Lee, J.H. Lee, I.-S. Lee, Toxicol. Res. 33 (2017) 97; (b) A. Salminen, M. Lehtonen, T. Suuronen, K. Kaarniranta, J. Huuskonen, Cell. Mol. Life Sci. 65 (2008) 2979:
 - (c) K.H. Wagner, I. Elmadfa, Ann. Nutr. Metab. 47 (2003) 95.
- [18] G. Wang, W. Tang, R.R. Bidigare, in: L. Zhang, A.L. Demain (Eds.), Natural Products: Drug Discovery and Therapeutic Medicine, Humana Press, Totowa,

- NJ, 2005, pp. [197]-[227].
- [19] D. Ciez, K. Kozieł, B. Horvath, J. Svetlik, Monatsh. Chem. 149 (2018) 1849.
- [20] J.D. Roberts, J.A. Yancey, J. Am. Chem. Soc. 75 (1953) 3165.
- [21] F.A. Carey, R.J. Sundberg, Advanced Organic Chemistry, Part A: Structure and Mechanisms, fifth ed., Springer Science, New York, 2007, pp. 1005–1007.
- [22] G.K. Friestad, in: M. Heinrich, A. Gansäuer (Eds.), Radicals in Synthesis III (Topics in Current Chemistry 320), Springer Verlag: Berlin Heidelberg, 2012, pp. [63]-[64].
- K.B. Wiberg, I. Org. Chem. 77 (2012) 10393.
- [24] Rigaku-Oxford Diffraction, CrysAlisPro Oxford Diffraction Ltd, Abingdon, England, 2006, V 1.171, 36, 2, (release 27-06-2012 CN).
- [25] M.C. Burla, R. Caliandro, M. Camalli, B. Carrozzini, G.L. Cascarano, L. De Caro, C. Giacovazzo, G. Polidori, R. Spagna, J. Appl. Crystallogr. 38 (2005) [381].
- [26] G.M. Sheldrick, Acta Crystallogr. A64 (2008) 112.
- [27] L.J. Farrugia, J. Appl. Crystallogr. 32 (1999) 837.
 [28] C.F. Macrae, P.R. Edgington, P. McCabe, E. Pidcock, G.P. Shields, R. Taylor,
- M. Towler, J. van de Streek, J. Appl. Crystallogr. 39 (2006) 453.

 [29] M.J. Frisch, G.W. Trucks, H.B. Schlegel, G.E. Scuseria, M.A. Robb, J.R. Cheeseman, G. Scalmani, V. Barone, B. Mennucci, G.A. Petersson, H. Nakatsuji, M. Caricato, X. Li, H.P. Hratchian, A.F. Izmaylov, J. Bloino, G. Zheng, J.L. Sonnenberg, M. Hada, M. Ehara, K. Toyota, R. Fukuda, J. Hasegawa, M. Ishida, T. Nakajima, Y. Honda, O. Kitao, H. Nakai, T. Vreven, J.A. Montgomery Jr., J.E. Peralta, F. Ogliaro, M. Bearpark, J.J. Heyd, E. Brothers, K.N. Kudin, V.N. Staroverov, R. Kobayashi, J. Normand, K. Raghavachari, A. Rendell, J.C. Burant, S.S. Iyengar, J. Tomasi, M. Cossi, N. Rega, J.M. Millam, M. Klene, J.E. Knox, J.B. Cross, V. Bakken, C. Adamo, J. Jaramillo, R. Gomperts, R.E. Stratmann, O. Yazyev, A.J. Austin, R. Cammi, C. Pomelli, J.W. Ochterski, R.L. Martin, K. Morokuma, V.G. Zakrzewski, G.A. Voth, P. Salvador, J.J. Dannenberg, S. Dapprich, A.D. Daniels, O. Farkas, J.B. Foresman, J.V. Ortiz, J. Cioslowski, D.J. Fox, Gaussian 09, Revision A.02, Gaussian, Inc, Wallingford, 2009
- [30] C. Gonzalez, H.B. Schlegel, J. Chem. Phys. 90 (1989) 2154.
- [31] A.D. Becke, J. Chem. Phys. 98 (1993) 1372.
- [32] J.D. Chai, M. Head-Gordon, Phys. Chem. Chem. Phys. 10 (2008) 6615.
- [33] Y. Zhao, D.G. Truhlar, Theor. Chem. Acc. 120 (2008) 215.
- J. Tomasi, B. Mennucci, R. Cammi, Chem. Rev. 105 (2005) 2999.
- [35] C. Møller, M.S. Plesset, Phys. Rev. 46 (1934) 618.
- [36] H.B. Schlegel, J. Chem. Phys. 84 (1986) 4530.
- [37] I. Mayer, Quantum Chem. 12 (1980) 189.
- [38] A.E. Reed, R.B. Weinstock, F. Weinhold, J. Chem. Phys. 83 (1985) 735.